The Effects of Hydrophobic Mismatch between Phosphatidylcholine Bilayers and Transmembrane α-Helical Peptides Depend on the Nature of Interfacially Exposed Aromatic and Charged Residues†

Maurits R. R. de Planque,*,‡,§ Jan-Willem P. Boots,‡ Dirk T. S. Rijkers,|| Rob M. J. Liskamp,|| Denise V. Greathouse,⊥ and J. Antoinette Killian*,‡

Center for Biomembranes and Lipid Enzymology, Institute of Biomembranes, Department of Biochemistry of Membranes, Utrecht University, Padualaan 8, 3584 CH Utrecht, The Netherlands, Department of Medicinal Chemistry, Utrecht University, Sorbonnelaan 16, 3584 CA Utrecht, The Netherlands, and Department of Chemistry and Biochemistry, University of Arkansas, Fayetteville, Arkansas 72701

Received March 4, 2002; Revised Manuscript Received April 26, 2002

ABSTRACT: In this study, we investigated the extent to which different aromatic and positively charged side chains, which often flank transmembrane segments of proteins, can influence lipid−peptide interactions. Model systems consisting of phosphatidylcholine and hydrophobic α-helical peptides with different flanking residues were investigated. The peptides were incorporated in relatively thick and in relatively thin lipid bilayers to create a peptide−bilayer hydrophobic mismatch, and the compensating effects on lipid structure were analyzed. When relatively long with respect to the thickness of the bilayer, the peptides that are flanked by the aromatic side chains, Trp, Tyr, and Phe, all induce a significant ordering of the lipid acyl chains, while the peptides flanked by the charged residues Lys, Arg, and His do not. However, when the peptides are relatively short with respect to the thickness of the bilayer, their effect on lipid organization does not depend primarily on their aromatic or charged character. Peptides flanked by Trp, Tyr, Lys, or (at low pH) His residues are effective in inducing mismatch-relieving cubic and inverted hexagonal phases, while analogues flanked by Phe, Arg, or (at neutral pH) His residues cannot induce an inverted hexagonal phase. The different responses to mismatch might reflect the different interfacial affinities of the residues that were investigated.

Three-dimensional structures of integral membrane proteins, helical bundles as well as β-barrels, generally show distinct belts of aromatic and charged residues on both sides of the membrane-spanning segments (*1*−*5*). Furthermore, analyses of the much larger number of protein sequences demonstrate that the predominantly hydrophobic stretches of ∼20 hydrophobic residues that represent putative transmembrane helices are preferentially flanked by aromatic and charged residues (*6*, *7*). It is estimated that in membranes the hydrophobic stretch is approximately aligned with the lipid acyl chains, while the aromatic and charged residues are in contact with the lipid headgroup regions on each side of the lipid bilayer. It has been proposed that it is energetically favorable for a membrane system to experience such a match between peptide hydrophobic length and bilayer hydrophobic thickness, and that the tendency to avoid hydrophobic mismatch is a director of membrane organization (*8*−*10*). It has also been postulated that the aromatic and charged residues have a specific affinity for the membrane−water interface, and that a need to avoid exposure of these residues to either excessively hydrophobic or excessively polar bilayer regions contributes to peptide−lipid interactions (*11*−*14*).

Model membrane systems consisting of phospholipids and synthetic polyleucine(alanine) transmembrane peptides have been used extensively to address the relationship between hydrophobic matching and membrane organization. It has been demonstrated that in phosphatidylcholine (PC) bilayers, the extent of incorporation of Lys-flanked and Trp-flanked analogues depends on the difference between peptide length and bilayer thickness (*15*−*17*). When this difference is not too large, the peptides remain incorporated in the bilayer. In this case, a peptide−bilayer mismatch induces (dis)-ordering of the flexible lipid acyl chains (*18*, *19*) or, at higher peptide concentrations and for negative mismatch situations, transitions to nonlamellar lipid phases, with the type of phase depending on the extent of mismatch (*20*). The effect of these lipid adaptations is that the hydrophobic bilayer thickness is adjusted so that a better match with the peptide hydrophobic length is obtained.

However, analogous Lys-flanked and Trp-flanked peptides with the same total length induce membrane rearrangements in PC to different extents (*21*). Additionally, peptides that

† This work was supported by the Council for Chemical Sciences (CW) with financial aid from the Netherlands Organization for Scientific Research (NWO) and by NIH Grant GM 34968 (to D.V.G.).

* To whom correspondence should be addressed. E-mail: m.r.r.deplanque@chem.uu.nl and j.a.killian@chem.uu.nl.

‡ Department of Biochemistry of Membranes, Utrecht University.

§ Present address: Department of NMR Spectroscopy, Bijvoet Center for Biomolecular Research, Utrecht University, Padualaan 8, 3584 CH Utrecht, The Netherlands.

|| Department of Medicinal Chemistry, Utrecht University.

⊥ University of Arkansas.

10.1021/bi0257686 CCC: $22.00
Published on Web 06/08/2002

are flanked by Lys as well as by Tyr or Phe residues have incorporation properties different from those of peptides that are flanked only by Lys residues, although these different peptides are similar in hydrophobic length (*22*). These observations indicate that in phosphatidylcholine model membranes, peptide−lipid interactions are not only modulated by a tendency to avoid a hydrophobic mismatch situation. Apparently, the nature of the flanking residues also contributes to the peptide−lipid interactions, possibly through (different) interactions of these aromatic and charged residues with the membrane−water interface.

In the study presented here, we have systematically investigated the influence of different aromatic and charged flanking residues on the lipid-modulating properties of a series of mismatching peptides in PC. When relatively long with respect to the thickness of the bilayer, the peptides that are flanked by the aromatic side chains, Trp, Tyr, and Phe, all induce a significant ordering of the lipid acyl chains, while the peptides flanked by the charged residues Lys, Arg, and His do not. However, when the peptides are relatively short with respect to the thickness of the bilayer, their ability to induce mismatch-relieving nonlamellar phases does not depend primarily on their aromatic or charged character. These results emphasize that the flanking residues contribute significantly to peptide−lipid interactions.

MATERIALS AND METHODS

Materials

All phospholipids were purchased from Avanti Polar Lipids Inc. (Birmingham, AL). WALP[1] and KALP peptides were synthesized and analyzed by analytical HPLC and electrospray mass spectrometry as described previously (*21*, *23*). The peptides with other aromatic and charged side chains were synthesized using the method employed for the KALP analogues, except for the treatment after the coupling reaction. These peptides were cleaved from the resin and deprotected by treatment with a trifluoroacetic acid/water/triisopropylsilane mixture (95:2.5:2.5, v/v/v) at room temperature for 3 h, except HALP23, which was treated with a trifluoroacetic acid/water/1,2-ethanedithiol mixture (95:2.5:2.5, v/v/v). RALP23, HALP23, and K′ALP23 were precipitated at −20 °C with a diethyl ether/hexane mixture (1:1, v/v) and YALP21 and FALP21 with a methyl *tert*-butyl ether/hexane mixture (1:1, v/v). The precipitates were decanted, subsequently washed three times with cold diethyl ether, and finally lyophilized from a *tert*-butanol/water mixture (1:1, v/v). W′ALP21 was precipitated in ice-cold water. The peptidic precipitates were collected by filtration, thoroughly washed with water, and finally dried over phosphorus pentoxide in a vacuum desiccator. Peptide purity was found to be >90% according to analytical HPLC. The identity of the peptides was confirmed by electrospray mass spectrometry.

Methods

Sample Preparation. Peptides, quantified by their dry weight, were predissolved in 10 μL of trifluoroacetic acid/mg of peptide and, after evaporation of the solvent by a stream of nitrogen, were dissolved in 1 mL of trifluoroethanol, followed by drying in a rotary evaporator. This step was repeated once. Next, the peptides were again dissolved in 0.5 mL of trifluoroethanol and added to 0.5 mL of a lipid suspension in distilled water, at temperatures above the gel to liquid crystalline phase transition, followed by addition of 10 mL of water and immediate lyophilization as described previously (*21*).

Lipid/peptide mixtures with a 1:10 peptide:lipid molar ratio (containing 20 μmol of lipid) were hydrated in 1.5 mL of buffer [100 mM NaCl and 25 mM Tris (pH 7.4)]. Samples were centrifuged (30000*g* for 15 min at 4 °C), and the supernatant was removed. Pellets were washed with buffer until the pH of the supernatant had reached the desired value. Next, the pellets were resuspended in 200 μL of buffer and subjected to 10 freeze−thaw cycles to equilibrate the sample. Samples containing HALP peptides were hydrated with different buffers to influence the protonation state of the His side chain. MES buffers [100 mM NaCl and 25 mM MES (pH 4.0 or 5.4)] were used to prepare samples at low pH values and Tris buffers [100 mM NaCl and 25 mM Tris (pH 7.4 or 8.9)] to prepare samples at higher pH values. Further sample preparation was identical to the general procedure described above.

Circular Dichroism Spectroscopy. CD samples of pure peptide were prepared by adding 1 mL of buffer [100 mM NaCl and 25 mM Tris (pH 7.4)] to 1 μmol of peptide powder. These samples were subsequently vortexed, sonicated for 30 min in a bath sonicator, and centrifuged (30000*g* for 15 min at 4 °C). For all peptides, this procedure resulted in a compact pellet and a clear supernatant, and CD spectra of the supernatant fraction were recorded. Lipid/peptide mixtures with a 1:30 peptide:lipid molar ratio (containing 7.5 μmol of lipid) were prepared as described above and were hydrated in 1 mL of buffer. These samples were then sonicated (5 min, 50% duty cycle, input power of 40 W, Branson 250 tip sonicator). To pellet down titanium particles and any residual multilamellar lipid structures, the sonicated samples were next centrifuged (30000*g* for 15 min at 4 °C). For all samples, CD measurements were carried out on a Jasco J-600 spectropolarimeter (0.2 mm path length cell, 1 nm bandwidth, 0.2 nm resolution, 1 s response time, scan speed of 20 nm/min, and 34 °C).

^{31}P NMR Measurements. ^{31}P NMR spectra of the peptide/lipid dispersions were recorded on a Bruker MSL300 NMR spectrometer. The sample temperature was regulated using a Bruker B-VT1000 temperature controller. Proton-decoupled experiments were carried out at 121.5 MHz (17 μs 90° pulse,

[1] Abbreviations: CD, circular dichroism; NMR, nuclear magnetic resonance; EM, electron microscopy; Etn, ethanolamine; Ac, acetyl; Tris, tris(hydroxymethyl)aminomethane; MES, 2-(*N*-morpholino)ethanesulfonic acid; W′, 1-methyltryptophan; K′, 2,3-diaminopropionic acid; WALP, tryptophan-alanine-leucine peptide Ac-GW$_2$(LA)$_n$W$_2$A-Etn; W′ALP21, 1-methyltryptophan-alanine-leucine peptide Ac-GW′$_2$(LA)$_7$LW′$_2$A-amide; YALP21, tyrosine-alanine-leucine peptide Ac-GY$_2$(LA)$_7$LY$_2$A-amide; FALP21, phenylalanine-alanine-leucine peptide Ac-GF$_2$(LA)$_7$LF$_2$A-amide; KALP23, lysine-alanine-leucine peptide Ac-GK$_2$(LA)$_8$LK$_2$A-amide; K′ALP23, 2,3-diaminopropionic acid-alanine-leucine peptide Ac-GK′$_2$(LA)$_8$LK′$_2$A-amide; RALP23, arginine-alanine-leucine peptide Ac-GR$_2$(LA)$_8$LR$_2$A-amide; HALP23, histidine-alanine-leucine peptide Ac-GH$_2$(LA)$_8$LH$_2$A-amide; PC, phosphatidylcholine; 14:0-PC, 1,2-dimyristoyl-*sn*-glycero-3-phosphocholine; 20:1$_c$-PC, 1,2-dieicosenoyl-*sn*-glycero-3-phosphocholine; 22:1$_c$-PC, 1,2-dierucoyl-*sn*-glycero-3-phosphocholine; 24:1$_c$-PC, 1,2-dinervonoyl-*sn*-glycero-3-phosphocholine; L$_\alpha$, liquid crystalline bilayer phase; I, isotropic phase; H$_{II}$, inverse hexagonal phase.

Table 1: Amino Acid Sequences of Peptides Flanked by Different Aromatic and Charged Residues, with Side Chain Structures Depicted

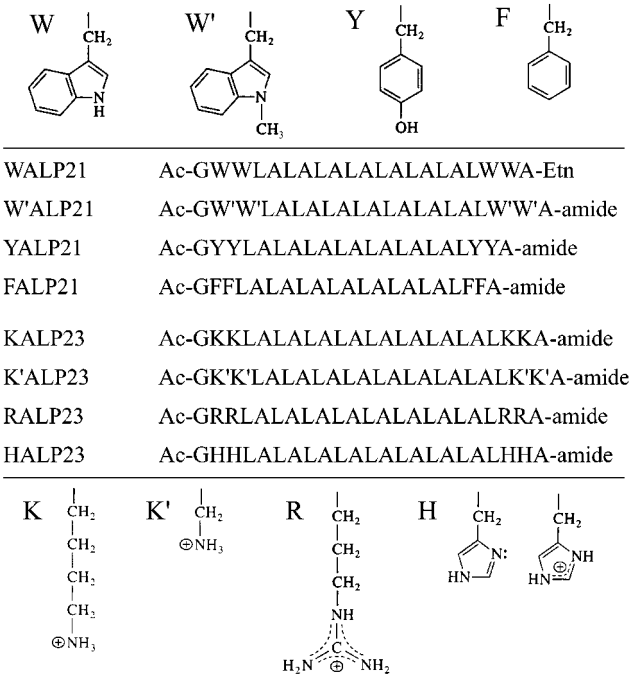

WALP21	Ac-GWWLALALALALALALALWWA-Etn
W'ALP21	Ac-GW'W'LALALALALALALALW'W'A-amide
YALP21	Ac-GYYLALALALALALALALYYA-amide
FALP21	Ac-GFFLALALALALALALALFFA-amide
KALP23	Ac-GKKLALALALALALALALALKKA-amide
K'ALP23	Ac-GK'K'LALALALALALALALALK'K'A-amide
RALP23	Ac-GRRLALALALALALALALALRRA-amide
HALP23	Ac-GHHLALALALALALALALALHHA-amide

1.3 s interpulse time, gated proton−noise decoupling). Approximately 15 000 scans were acquired, and a sweep width of 25 kHz and 1024 complex data points were used. Prior to Fourier transformation, an exponential multiplication was applied, resulting in a 100 Hz line broadening. The chemical shift was referenced to a sample with isotropically moving PC molecules. All spectra were scaled to the same height.

^{2}H NMR Measurements and Analysis. Samples containing peptide and 15 μmol of *sn*-2 perdeuterated 14:0-PC at a 1:30 molar ratio were hydrated in 1 mL of deuterium-depleted water. The samples were centrifuged (30000*g* for 15 min at 4 °C), and the supernatant was removed. The pellet was washed with deuterium-depleted water if the pH of the supernatant was below 6. ^{2}H NMR spectra of the pellets were recorded on a Varian Unity400+ NMR spectrometer at 34 °C, using a broadband probe with a 10 mm solenoidal sample coil. ^{2}H NMR measurements were performed at 61.4 MHz, using a quadrupolar echo sequence (*24*) (12 μs 90° pulse and 30 μs pulse separation), a repetition rate of two acquisitions per second, and a spectral width of 100 kHz, with 2880 complex data points in the time domain. Approximately 100 000 scans were accumulated. The free induction decays were left-shifted to begin at the top of the echo, zero-filled to 8192 points, and multiplied with an exponential window function equivalent to a line broadening of 100 Hz. Unsymmetrized ^{2}H NMR powder spectra were analyzed by dePakeing as described previously (*18*). This procedure results in spectra that would be obtained for an aligned membrane with its bilayer normal parallel to the magnetic field. It enhances the resolution and results in doublets with splittings $\Delta\nu_Q$ that relate to the segmental order parameter $S(i)$. Order parameter profiles were obtained by assuming that the segmental order varies monotonically along the acyl chain from the C^3D_2 to the $C^{14}D_3$ moiety. From the order parameter profiles, the effective length of the acyl chains was estimated and extrapolated to the hydrophobic bilayer thickness as described previously (*18*).

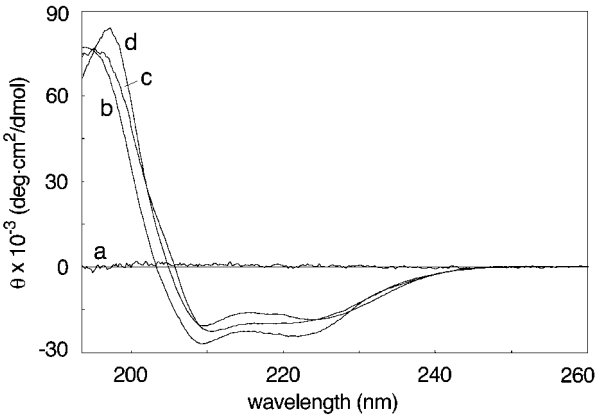

FIGURE 1: Circular dichroism spectra of peptides in aqueous solution, in the absence (a) and presence (b−d) of 14:0-PC: WALP21 (b), YALP21 (a and c), and FALP21 (d), at a 1:30 peptide:lipid molar ratio.

Freeze-Fracture Electron Microscopy. Peptide/lipid samples previously used for ^{31}P NMR measurements were, after incubation at the desired temperature, sandwiched between two hat-shaped copper holders, and rapidly frozen in liquid nitrogen-cooled propane using a KF80 plunge freezing device (Reichert Jung, Vienna, Austria). After fracturing had been carried out, platinum−carbon replicas were made in a BAF400 apparatus (Bal-tec, Baltzers, Liechtenstein). Replicas were observed with a Philips CM10 electron microscope operated at 80 kV.

RESULTS

Lipid-Modulating Properties of Peptides with Aromatic Flanking Residues. The lipid interactions of relatively short or relatively long transmembrane peptides that are flanked by tryptophans (WALP peptides) have been characterized extensively (*17*, *18*, *20*, *21*). In the study presented here, we compared the lipid-modulating properties of the WALP peptides with the effects of analogues with other aromatic residues or with charged residues.

First, the conformational behavior and membrane-associating properties of the WALP21, YALP21, and FALP21 peptides (Table 1) were characterized by circular dichroism (CD) spectroscopy. In the absence of lipid, no significant signal was observed for any of the three analogues, as shown in Figure 1 for YALP21 (curve a). This indicates that the peptides are insoluble in aqueous solution. Consequently, the spectra in the presence of 14:0-PC correspond exclusively to the membrane-incorporated peptide (*17*, *21*). The line shape of these spectra, characterized by minima near 222 and 208 nm and a maximum near 190 nm, is indicative of a predominantly α-helical conformation for each peptide (*25*), and as judged from the intensities of the corresponding spectra, the three peptides associate completely with 14:0-PC bilayers.

The effects of these peptides on bilayer thickness were characterized under positive mismatch conditions. The ^{2}H NMR spectra of 14:0-PC dispersions in the absence and presence of the peptides are presented in Figure 2. It can be seen that relative to pure 14:0-PC (spectrum a), incorporation

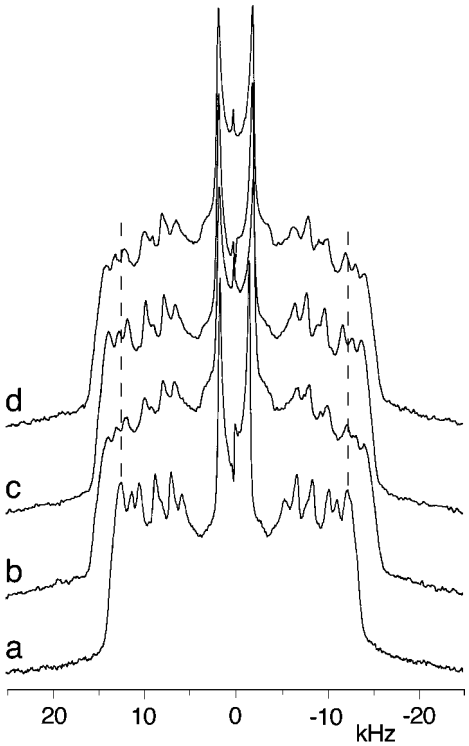

FIGURE 2: ^{2}H NMR spectra of dispersions of 14:0-PC-d_{27} in the absence (a) and presence of the following peptides: WALP21 (b), YALP21 (c), and FALP21 (d), at a 1:30 peptide:lipid molar ratio.

Table 2: Changes in Mean Hydrophobic Thickness (Δd) Relative to the Thickness of Pure *sn*-2 Chain Perdeuterated 14:0-PC (22.5 Å), for Systems at a 1:30 Peptide:Lipid Molar Ratio[a]

peptide	Δd (Å)	peptide	Δd (Å)	peptide	Δd (Å)
WALP16	0.4[b]	WALP21	0.8	KALP23	0.2[b]
WALP19	0.6[b]	YALP21	0.7	RALP23	0.2
WALP23	1.0[b]	FALP21	0.8	HALP23	0.2

[a] Measurements were performed at 34 °C, 10 °C above the main phase transition temperature of pure 14:0-PC. The estimated experimental precision in hydrophobic thickness is ±0.1 Å. [b] Value obtained from ref *21*.

of WALP21 (b), YALP21 (c), or FALP21 (d) increases the quadrupolar splittings for the central methyl and the outer methylene peaks. Visual inspection of the spectra reveals that the three peptides induce almost identical increases in spectral width. Resolution-enhancing dePakeing analysis (see Methods) was applied to quantify the peptide-induced ordering of the lipid acyl chains. The WALP, YALP, and FALP analogues were found to increase the quadrupolar splittings of the outer methylene peaks, with respect to those of pure 14:0-PC, with 3.2, 2.8, and 3.0 kHz, respectively. The splittings corresponding to the terminal methylene and methyl moieties are also increased, but to a progressively lesser extent. For the different systems, order parameter profiles were obtained, the shape of which was similar in the absence and presence of the peptides, as demonstrated previously for different WALP analogues (*18*). From these order parameter profiles, it was estimated that WALP21 causes an increase of 0.8 Å in mean hydrophobic bilayer thickness, a value between those previously obtained for WALP19 and WALP23 (see Table 2). For the YALP21 and FALP21 analogues, increases of 0.7 and 0.8 Å, respectively, are obtained. Thus, the three peptides exhibit similar effects on the chain order of 14:0-PC, indicating that they increase the bilayer thickness to the same extent.

The analogues were next incorporated in relatively thick bilayers of 20:1$_c$-, 22:1$_c$-, and 24:1$_c$-PC, to investigate their ability to influence lipid organization under negative mismatch conditions. We recorded ^{31}P NMR spectra of the different peptide/lipid dispersions at 60 °C to allow optimal expression of nonlamellar phases, as described previously for WALP and KALP analogues (*21*). As shown in Figure 3, pure PC dispersions give a ^{31}P NMR spectrum with a low-field shoulder and a high-field peak, typical for the preferred planar bilayer organization in the liquid crystalline (L_α) phase (*26*, *27*). In contrast, all of the peptide-containing systems display nonlamellar spectral components. The spectra for WALP21 in 20:1$_c$- and 22:1$_c$-PC consist of an isotropic (I) signal that has been ascribed to a cubic lipid phase (*20*). In the longest lipid, 24:1$_c$-PC, an H_{II} phase is formed, as characterized by the spectral component with a peak which is low-field to that of the isotropic position with inverted asymmetry (*26*, *27*). This phase is formed presumably because the mismatch has become too large for the peptide to be accommodated in the isotropic phase (*20*). Similar behavior is observed for YALP21. Also, FALP21 induces an isotropic phase in the shorter chain lipids. However, unlike WALP21 and YALP21, FALP21 does not induce an H_{II} phase in the longest chain lipid. Instead, the spectrum of FALP21 in 24:1$_c$-PC consists of an L_α component, on which a broad isotropic spectral contribution is superimposed.

This difference between the effects on 24:1$_c$-PC phase behavior of FALP21 on one hand and of WALP21 and YALP21 on the other hand could be related to the fact that the Trp and Tyr side chains can participate in hydrogen bonds, whereas Phe cannot. This possibility was addressed by synthesizing a peptide that is flanked by indole N-methylated Trp residues (see Table 1), which also cannot form hydrogen bonds. The corresponding W′ALP21 peptide can induce nonlamellar phases, and the type of nonlamellar phase that is formed is the same as for WALP21 (Figure 3). However, the methylated analogue is less efficient in inducing H_{II} phase formation than WALP21 or YALP21. These results show that the hydrogen bonding of indole is not an essential factor for induction of nonlamellar phases.

To gain insight into the macroscopic lipid organization that gives rise to the various spectra, freeze-fracture electron microscopy (EM) was used on selected peptide/lipid systems that were incubated at 60 °C prior to rapid freezing. In the fracture plane of WALP21/20:1$_c$-PC (Figure 4A) and FALP21/20:1$_c$-PC (Figure 4B) samples, extended two-dimensional domains of closely packed spheres with diameters of 25−30 and 15−20 nm, respectively, were observed. This morphology corresponds to a cubic lipid phase (*28*), consistent with the interpretation of the narrow isotropic ^{31}P NMR signal of systems with shorter WALP peptides (*20*). In the WALP21/24:1$_c$-PC sample, parallel running tubes with an estimated diameter of ∼10 nm were observed (Figure 4C), which, consistent with the characteristic ^{31}P NMR spectrum of this sample, represents the morphology of the H_{II} phase (*28*). The broad isotropic component of the ^{31}P NMR spectrum of FALP21 in 24:1$_c$-PC could not be related to a well-defined macroscopic peptide/lipid organization. EM analysis of this sample showed multilamellar vesicles with

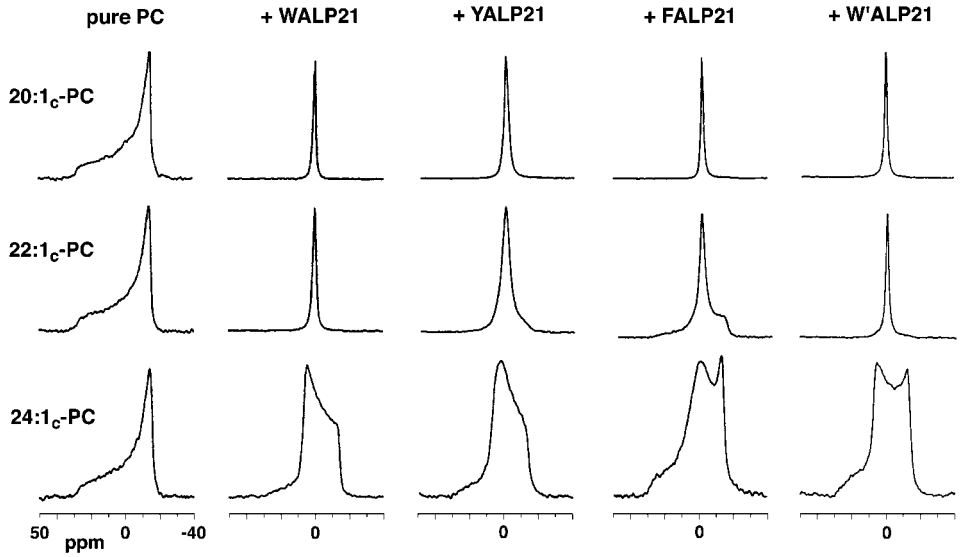

FIGURE 3: ^{31}P NMR spectra of dispersions of 20:1$_c$-, 22:1$_c$-, and 24:1$_c$-PC, in the absence and presence of WALP21, YALP21, FALP21, and W′ALP21, as indicated in the figure, at a 1:10 peptide:lipid molar ratio.

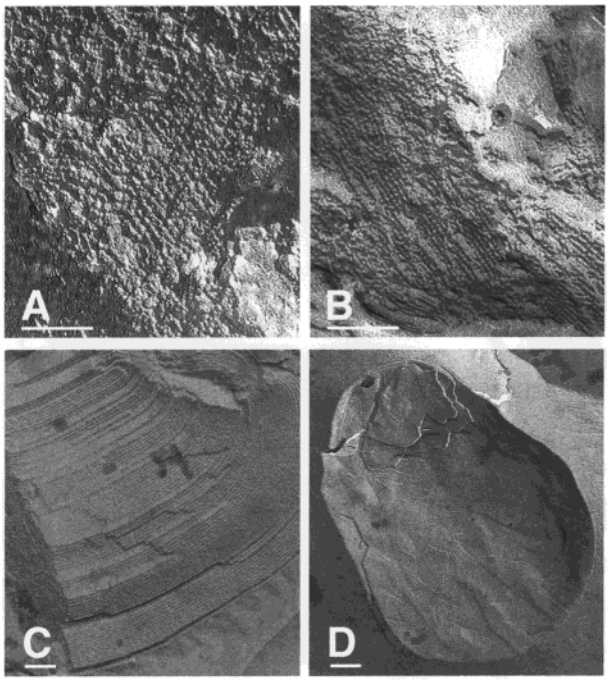

FIGURE 4: Peptide/lipid systems, at a 1:10 peptide:lipid molar ratio, as visualized by freeze-fracture EM: (A) WALP21/20:1$_c$-PC, (B) FALP21/20:1$_c$-PC, (C) WALP21/24:1$_c$-PC, and (D) FALP21/24:1$_c$-PC. Bars are 100 nm in length.

line-shaped defects, with a width of ~3 nm, in the plane of the bilayers (Figure 4D). These defects probably consist of areas with a relatively high degree of curvature that will enable an increased motional averaging of the ^{31}P NMR signal, thereby giving rise to a broad isotropic ^{31}P NMR signal. The observed defects might resemble the bilayer distortions around peptide line aggregates that have been postulated in a recent AFM study on WALP peptides in supported gel state bilayers (*29*).

Lipid-Modulating Properties of Peptides with Charged Flanking Residues. Lys-flanked KALP, Arg-flanked RALP, and His-flanked HALP peptides (Table 1) were synthesized, and their lipid-modulating properties were investigated under conditions of positive and negative mismatch. A total peptide

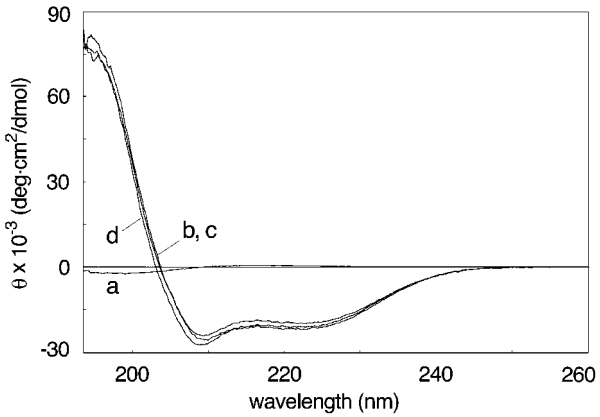

FIGURE 5: Circular dichroism spectra of peptides in aqueous solution, in the absence (a) and presence (b−d) of 14:0-PC: KALP23 (b), RALP23 (a and c), and HALP23 (d), at a 1:30 peptide:lipid molar ratio.

length of 23 residues was selected because shorter KALP analogues are too polar to incorporate in bilayers under mismatch conditions, and because WALP21 and KALP23 have similar effects in relatively thick bilayers (*21*). First, CD spectra were recorded in the presence and absence of 14:0-PC to assess the conformational behavior and membrane-associating properties of KALP23, RALP23, and HALP23. As shown in Figure 5 for RALP23, the peptides do not give rise to a significant CD signal in an aqueous salt solution (curve a), indicating that the signal observed in the presence of 14:0-PC corresponds to the incorporated peptide. The spectral line shape and intensity for KALP23 (b), RALP23 (c), and HALP23 (d) demonstrate that the peptides adopt an α-helical conformation (*25*) and are totally incorporated in the 14:0-PC bilayer (*21*).

Despite quantitative incorporation of the peptides in 14:0-PC, ^{2}H NMR spectra of bilayers of *sn*-2 perdeuterated 14:0-PC in the presence and absence of peptide are very similar (see Figure 6), suggesting that the peptides do not have a significant effect on the acyl chain order. Analysis of the ^{2}H NMR data shows that incorporation of KALP23, RALP23, or HALP23 causes an increase in the outer methylene quadrupolar splitting of only 0.8 kHz on average, and

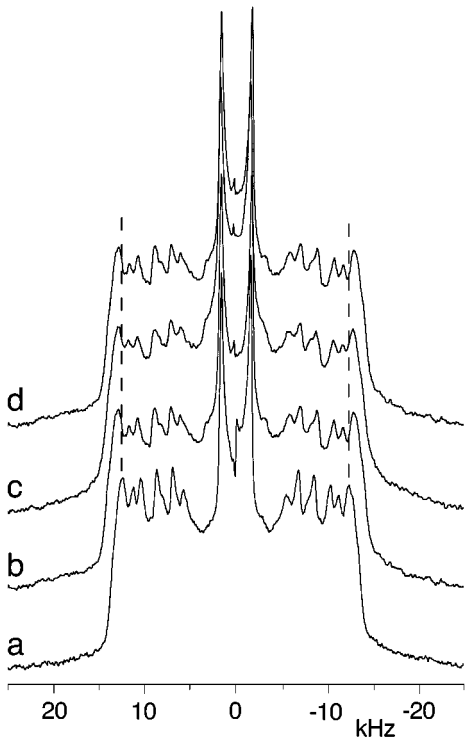

FIGURE 6: ^{2}H NMR spectra of dispersions of 14:0-PC-d_{27} in the absence (a) and presence of the following peptides: KALP23 (b), RALP23 (c), and HALP23 (d), at a 1:30 peptide:lipid molar ratio.

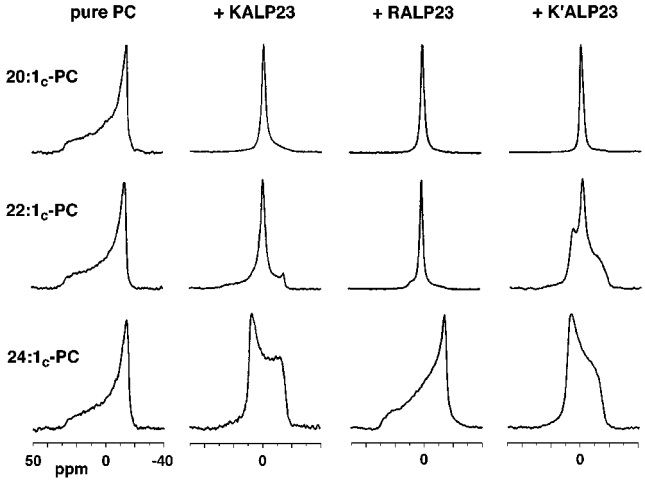

FIGURE 7: ^{31}P NMR spectra of dispersions of 20:1$_c$-, 22:1$_c$-, and 24:1$_c$-PC, in the absence and presence of KALP23, RALP23, and K′ALP23, as indicated in the figure, at a 1:10 peptide:lipid molar ratio.

increases the mean hydrophobic thickness by no more than 0.2 Å (Table 2).

The effects of KALP23 and RALP23 were also investigated under conditions of negative mismatch. As shown in Figure 7, Lys-flanked KALP23 induces isotropic and H_{II} nonlamellar phases, with an $I \rightarrow H_{II}$ transition between 22:1$_c$- and 24:1$_c$-PC. Although Arg-flanked RALP23 also induces an isotropic phase in 20:1$_c$- and 22:1$_c$-PC, it does not induce an $I \rightarrow H_{II}$ transition with an increasing level of mismatch. Instead, a pure L_α phase is observed in 24:1$_c$-PC. This behavior resembles the membrane-modulating properties of Phe-flanked FALP21.

To investigate whether the strong membrane-modulating properties of KALP23 are imposed exclusively by the charged ϵ-NH_3^+ moiety of the Lys side chain, a peptide was synthesized with flanking groups that are three methylene groups shorter than the Lys side chain (Table 1). This K′ALP23 analogue has an effect on lipid phase behavior similar to that of KALP23 (Figure 7), but it induces an H_{II} phase in shorter lipids. This indicates that the removal of three methylene groups from the Lys side chain does not influence the membrane-modulating properties of KALP23, but rather decreases its effective hydrophobic length.

Because the charge on His side chains changes with pH, HALP23 (Table 1) can be used to study the relation between charge density and macroscopic lipid organization. Varying the environmental pH did not alter the preferred L_α organization of the pure lipid systems (data not shown). As depicted in Figure 8, incorporation of HALP23 at pH 8.9 results in the formation of an isotropic lipid phase in 20:1$_c$- and 22:1$_c$-PC, while 24:1$_c$-PC remains in an L_α phase, similar to that observed for RALP23. Gradually decreasing the environmental pH increases the amount of nonlamellar phase formed in all lipid systems. At pH 5.4, a small H_{II} component is visible in the ^{31}P NMR spectra of 24:1$_c$-PC. At pH 4.0, both the 24:1$_c$- and 22:1$_c$-PC systems display large amounts of the H_{II} phase (Figure 8), while 20:1$_c$-PC still forms an isotropic phase. Thus, at low pH, HALP23 behaves like K′ALP23, suggesting that charge density is an important determinant for mismatch-induced lipid adaptations.

DISCUSSION

Lipid-exposed transmembrane protein segments generally consist of a stretch of hydrophobic residues that is preferentially flanked on both sides by aromatic and charged residues (*5*, *6*). If the length of the (possibly tilted) hydrophobic segment matches the hydrophobic thickness of the bilayer, the flanking residues will be positioned near the lipid−water interface (*14*). The energy cost of a mismatch situation might be determined not only by hydrophobic mismatch considerations (reviewed in refs *8*−*10*) but possibly also by the interactions of flanking residues with the lipid−water interface. To gain insight into the influence of the flanking residues, we have investigated the effects of hydrophobic mismatch on lipid structure under conditions of both positive and negative mismatch, using a series of designed transmembrane peptides with different flanking residues (see Table 1).

Positive Mismatch Conditions. It has previously been observed that Trp-flanked peptides order the lipid acyl chains of a relatively thin PC bilayer to a significantly larger extent than Lys-flanked analogues (*21*). The ^{2}H NMR experiments described in the study presented here demonstrate that Tyr-flanked YALP and Phe-flanked FALP analogues order the acyl chains of 14:0-PC bilayers to approximately the same extent as analogous Trp-flanked WALP peptides, while Arg-flanked RALP and His-flanked HALP peptides have the same small effect as a Lys-flanked analogue. The increase in average bilayer thickness that is a result of the incorporation of the peptides that are flanked by aromatic residues indicates that these peptides are too long to be accommodated in an unperturbed 14:0-PC bilayer. In contrast, the peptides that are flanked by charged residues can be accommodated without a significant increase in bilayer thickness and, as previously shown for Lys-flanked peptides, without other

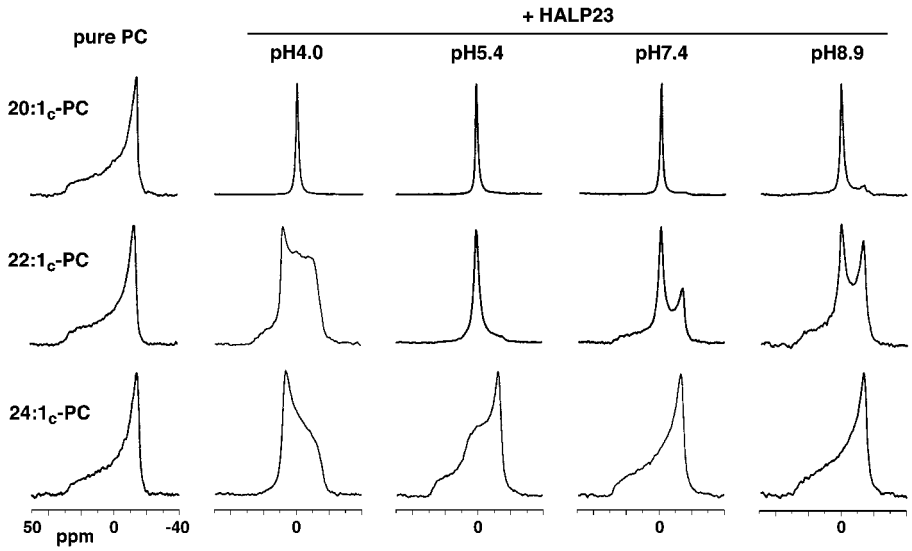

FIGURE 8: ^{31}P NMR spectra of dispersions of 20:1$_c$-, 22:1$_c$-, and 24:1$_c$-PC, in the absence and presence of HALP23 at environmental pH values of 4.0, 5.4, 7.4, and 8.9, as indicated in the figure, at a 1:10 peptide:lipid molar ratio.

likely compensating mechanisms, such as peptide aggregation (*21*, *30*) or a substantial peptide tilt (*31*, *32*). This is in spite of the fact that these peptides are two amino acids longer than the analogues that are flanked by aromatic residues.

These effects could be rationalized by assuming that peptides that are flanked by aromatic residues have a larger hydrophobic length than peptides that are flanked by the more polar charged residues. When for the latter peptides the hydrophobic length is defined as the length of the polyleucine-alanine stretch (in an ideal α-helical conformation) between the flanking residues, a value of 25.5 Å is obtained. The hydrophobic thickness of an unperturbed 14:0-PC bilayer is approximately 23 Å (*33*), and consequently, the peptides that are flanked by charged residues would experience only a small mismatch situation in 14:0-PC. However, analogues that are two amino acids shorter (with an estimated length of the polyleucine-alanine stretch of 22.5 Å) but are flanked with aromatic amino acids could have a larger hydrophobic length. This length could be up to 28.5 Å if one would consider the four flanking residues as part of the hydrophobic stretch. In this case, the analogues would experience a positive mismatch situation in 14:0-PC, which can be (partly) compensated by ordering of the lipid acyl chains (*18*).

As an alternative explanation, the effective hydrophobic length of the peptides could be modulated by a preference of the aromatic and charged side chains for distinct interfacial environments, which is not based only on hydrophobicity. Small water-soluble compounds that mimic the Trp and Tyr side chains have been shown by a fluorescence quenching approach to prefer localization at a relatively deep interfacial position, near the lipid carbonyl groups (*12*). For aromatic residues that are present on both termini of a transmembrane peptide, this location cannot be obtained on both sides of a bilayer when the separating stretch of amino acids is relatively long, and peptides such as WALP21 would consequently experience a positive mismatch situation in 14:0-PC. Charged residues are expected to favor a more polar interfacial location, closer to the aqueous phase. In this case, a longer separating stretch is favorable in positioning the charged side chains at the preferred shallow location on both sides of the bilayer, and therefore, peptides such as KALP23 would not experience a significant mismatch in bilayers of 14:0-PC.

Negative Mismatch Conditions. The long chain species 20:1$_c$-, 22:1$_c$-, and 24:1$_c$-PC have hydrophobic thicknesses of 30.5, 34.0, and 37.5 Å, respectively, at temperatures that are approximately 10 °C above their respective gel to liquid phase transition temperatures (*17*, *33*). Also at the higher temperature as used in our measurements, the hydrophobic length of the employed peptides, when defined as the length of the polyleucine-alanine stretch, can be expected to be significantly shorter than the hydrophobic thickness of the longer lipids. Under these negative mismatch conditions, WALP21, YALP21, and FALP21 all induce an isotropic (cubic) organization of 20:1$_c$-PC and 22:1$_c$-PC (Figure 3). Such formation of nonlamellar lipid phases can be understood on the basis of the fact that these phases contain areas of reduced thickness that enable relatively short peptides to be accommodated with little or no hydrophobic mismatch, as discussed previously (*20*). A cubic phase is not observed for the longest lipid, 24:1$_c$-PC, indicating that the reduction in "membrane" thickness offered by this phase is not sufficient to compensate for the mismatch. Instead, WALP21 and YALP21 induce a highly curved H_{II} phase, for which regions of reduced thickness apparently prevent situations of larger mismatch. Because phosphatidylcholine species strongly prefer organization in a lamellar phase (*34*, *35*), it is remarkable that, at high concentrations, mismatching peptides can induce formation of these highly curved nonlamellar phases. However, unlike "easier" mismatch responses such as aggregation, nonlamellar phase formation enables hydrophobic matching while at the same time the flanking residues remain in contact with the membrane−water interface (*20*).

In contrast to the Trp-flanked and Tyr-flanked analogues, the Phe-flanked analogue is not able to induce a well-defined mismatch-relieving phase in 24:1$_c$-PC, and therefore, this system probably responds to a large negative mismatch with other compensating mechanisms, such as the formation of peptide aggregates. Why do Phe-flanked peptides behave differently than analogues that are flanked by the other aromatic residues, Trp and Tyr? The observation that

FALP21, just as WALP21 and YALP21, induces a cubic phase in 20:1_c-PC and 22:1_c-PC but not in 24:1_c-PC indicates that the hydrophobic lengths of the peptides are the same. It is therefore likely that the different mismatch response of the 24:1_c-PC system is due to different interactions of the aromatic side chains with the interfacial region. We speculate that the FALP peptides are not as effective in inducing a mismatch-relieving H_{II} phase as the WALP and YALP analogues because for the Phe side chain, positioning into an interfacial environment is not as favorable as for the Trp and Tyr side chains, and therefore (partial), aggregation of FALP peptides (as suggested from the EM measurements) is an acceptable mismatch-relieving response.

The preference for an interfacial environment of water-soluble analogues of Trp and Tyr side chains has been explained by factors such as hydrogen bonding with water or interfacial lipid groups, dipolar interactions with lipid carbonyls, and cation$-\pi$ interactions (discussed in refs *36* and *37*). Therefore, the deviating response to mismatching FALP analogues could correlate with a lack of hydrogen bonding functionality of the Phe side chain. However, because W′ALP21, the flanking residues of which lack the hydrogen bonding function, induces isotropic phases in 20:1_c-PC and 22:1_c-PC, and an H_{II} phase in 24:1_c-PC, side chain hydrogen bonding is not absolutely required for the induction of a nonlamellar phase, although there are quantitative differences in the relative amount of H_{II} phase and in the width of the H_{II} signal. What other factors could explain the different properties of the Phe-flanked analogue? The size of the aromatic π-electron system is not likely to be decisive, since this is rather similar for Tyr and Phe, while YALP and FALP peptides interact differently with lipid bilayers. It is, however, noteworthy that the ability of the aromatic side chains to affect lipid organization does seem to correlate roughly with the magnitude of the dipole moment [values of 2.2, 1.6, and 0.4 D have been reported for indole, phenol, and methylbenzene, respectively (*38*, *39*)] of the aromatic side chain. A larger dipole moment might promote positioning of a side chain at the interface through favorable interactions with, for example, the dipole moments of the lipid carbonyl groups and/or the water molecules that are present in the interface.

When relatively short, the Lys-flanked KALP23 has the same effect on lipid phase behavior as WALP21, suggesting that these two peptides have the same effective hydrophobic length, in agreement with previous observations (*21*). The different length of the peptides was chosen to compare the H_{II} phase-inducing capacity of these peptides in the same lipids, thus eliminating possible lipid-specific effects.

Just like KALP23, the Arg-flanked RALP23 analogue induces an isotropic (cubic) lipid organization in 20:1_c- and 22:1_c-PC, while an isotropic ^{31}P NMR signal is not observed for the 24:1_c-PC system (Figure 7). Apparently, the two peptides have a similar effective hydrophobic length. However, in contrast to mismatching KALP23, RALP23 is unable to induce formation of a H_{II} phase, which might be attributed to different interfacial interactions of the Lys and Arg side chains. This is surprising because the positive charge is generally considered to impart similar properties to Lys and Arg. It could be that the substantial delocalization of the positive charge in the guanidinium group of Arg affects the ability of RALP23 to form a mismatch-relieving H_{II} phase in which the Arg side chains are exposed to an interfacial environment. That charge is an important determinant for H_{II} phase formation is supported by experiments with HALP23 as a function of pH. At low environmental pH, where the His side chain is positively charged, the peptide can induce H_{II} phase formation, while at higher pH, the peptide is unable to do so (Figure 8). We speculate that a higher charge density reduces the compatibility with the apolar environment of the hydrophobic core and therefore favors a mismatch response such as nonlamellar phase formation, in which hydrophobic matching can be combined with an interfacial positioning of the flanking residues. It can also be expected that a higher charge density on the side chains disfavors peptide aggregation as a mismatch response.

The observation that K′ALP23, in which $(CH_2)_4$ within the Lys side chains is shortened to CH_2 (Table 1), induces an H_{II} phase just as KALP23 indicates that the charged ϵ-NH_3^+ moiety of the Lys side chain is sufficient to impart strong lipid-modulating properties to KALP23. Moreover, the fact that K′ALP23 induces an H_{II} phase in shorter lipids than KALP23 indicates that the effective length of K′ALP23 is shorter than that of KALP23. This can be rationalized when the Lys side chains of KALP23 are present in an extended "snorkling" conformation along the helix axis, with the terminal ϵ-NH_3^+ moieties pointing outward in the direction of the aqueous phase (*40*, *41*). The RALP23 peptide would also be expected to be able to increase its effective hydrophobic length by snorkling of its long and flexible side chains, but this does not seem to be a likely option for the rigid His side chains. This might explain why RALP23 appears to have the same effective length as KALP23 but why the lipid-modulating properties of HALP23 at low pH are similar to those of K′ALP23.

It can be concluded that under negative mismatch conditions, the observed mismatch response in PC systems is modulated by the precise structure of the flanking residues. As shown in a related study, this is in striking contrast to the effects of the peptides in lipids which have an inherent tendency to form nonlamellar phases. In this case, all the peptides that are flanked by aromatic residues and all the peptides that are flanked by charged residues have similar effects, and only a difference in effective hydrophobic length between the two classes of peptides is evident (*42*). This underlines the suitability of PC systems for gaining insight into peptide$-$lipid interactions. For mismatching peptides in PC, the influence of flanking residue structure does not seem to be governed by hydrophobicity alone, and therefore, specific interactions with the interfacial region might be involved. Interestingly, Wimley and White developed an interfacial hydrophobicity scale by assessing the partitioning of unstructured pentapeptides that differ in the nature of a guest residue, between the aqueous phase and a PC bilayer surface (*43*). In general, they find a strong correlation between hydrophobicities derived from water-to-bilayer partitioning and from water-to-octanol partitioning, which indicates that membrane partitioning is driven mainly by the hydrophobic effect. However, some side chains, most notably, those of the aromatic and charged residues, deviate from this linear relationship, which Wimley and White attributed to specific interactions of these residues with the interface (*43*). For different side chains, the deviation from linearity is in the following order: Trp $\sim$ Tyr $>$ Lys $\sim$ Phe

> Arg ∼ His (uncharged). This approximately reflects the ability of mismatching peptides that are flanked by these residues to induce a mismatch-relieving H_{II} phase, supporting the notion that this is related to interfacial interactions of the aromatic and charged side chains.

We conclude that for the peptides and lipid systems employed in this study, interfacial interactions of the aromatic and charged flanking residues contribute significantly to peptide−lipid interactions.

ACKNOWLEDGMENT

We thank Drs. Roger E. Koeppe, II, Ben de Kruijff, and Tony Watts for helpful suggestions on the manuscript, Gerda de Korte for HPLC analysis, and Sebastiaan Wesseling for assistance with sample preparation and peptide synthesis.

REFERENCES

1. Doyle, D. A., Cabral, J. M., Pfuetzner, R. A., Kuo, A., Gulbis, J. M., Cohen, S. L., Chait, B. T., and MacKinnon, R. (1998) *Science 280*, 69−77.
2. Schulz, G. E. (1993) *Curr. Opin. Cell Biol. 5*, 701−707.
3. Ulmschneider, M. B., and Sansom, M. S. P. (2001) *Biochim. Biophys. Acta 1512*, 1−14.
4. Wallin, E., Tsukihara, T., Yoshikawa, S., Von Heijne, G., and Elofsson, A. (1997) *Protein Sci. 6*, 808−815.
5. Sakai, H., and Tsukihara, T. (1998) *J. Biochem. 124*, 1051−1059.
6. Arkin, I. T., and Brunger, A. T. (1998) *Biochim. Biophys. Acta 1429*, 113−128.
7. Landolt-Marticorena, C., Williams, K. A., Deber, C. M., and Reithmeier, R. A. F. (1993) *J. Mol. Biol. 229*, 602−608.
8. Mouritsen, O. G., and Bloom, M. (1993) *Annu. Rev. Biophys. Biomol. Struct. 22*, 145−171.
9. Killian, J. A. (1998) *Biochim. Biophys. Acta 1376*, 401−416.
10. Dumas, F., Lebrun, M. C., and Tocanne, J.-F. (1999) *FEBS Lett. 458*, 271−277.
11. Schiffer, M., Chang, C.-H., and Stevens, F. J. (1992) *Protein Eng. 5*, 213−214.
12. Kachel, K., Asuncion-Punzalan, E., and London, E. (1995) *Biochemistry 34*, 15475−15479.
13. Stopar, D., Spruijt, R. B., Wolfs, C. J. A. M., and Hemminga, M. A. (1996) *Biochemistry 35*, 15467−15473.
14. Killian, J. A., and Von Heijne, G. (2000) *Trends Biochem. Sci. 25*, 429−434.
15. Ren, J., Lew, S., Wang, Z., and London, E. (1997) *Biochemistry 36*, 10213−10220.
16. Webb, R. J., East, J. M., Sharma, R. P., and Lee, A. G. (1998) *Biochemistry 37*, 673−679.
17. De Planque, M. R. R., Goormaghtigh, E., Greathouse, D. V., Koeppe, R. E., II, Kruijtzer, J. A. W., Liskamp, R. M. J., De Kruijff, B., and Killian, J. A. (2001) *Biochemistry 40*, 5000−5010.
18. De Planque, M. R. R., Greathouse, D. V., Koeppe, R. E., II, Schäfer, H., Marsh, D., and Killian, J. A. (1998) *Biochemistry 37*, 9333−9345.
19. Nezil, F. A., and Bloom, M. (1992) *Biophys. J. 61*, 1176−1183.
20. Killian, J. A., Salemink, I., De Planque, M. R. R., Lindblom, G., Koeppe, R. E., II, and Greathouse, D. V. (1996) *Biochemistry 35*, 1037−1045.
21. De Planque, M. R. R., Kruijtzer, J. A. W., Liskamp, R. M. J., Marsh, D., Greathouse, D. V., Koeppe, R. E., II, De Kruijff, B., and Killian, J. A. (1999) *J. Biol. Chem. 274*, 20839−20846.
22. Mall, S., Broadbridge, R., Sharma, R. P., Lee, A. G., and East, J. M. (2000) *Biochemistry 39*, 2071−2078.
23. Greathouse, D. V., Goforth, R. L., Crawford, T., Van der Wel, P. C. A., and Killian, J. A. (2001) *J. Pept. Res. 57*, 519−527.
24. Davis, J. H., Jeffrey, K. R., Bloom, M., Valic, M. I., and Higgs, T. P. (1976) *Chem. Phys. Lett. 42*, 390−394.
25. Greenfield, N., and Fasman, G. D. (1969) *Biochemistry 8*, 4108−4116.
26. Seelig, J. (1978) *Biochim. Biophys. Acta 515*, 105−140.
27. Cullis, P. R., and De Kruijff, B. (1979) *Biochim. Biophys. Acta 559*, 399−420.
28. Meyer, H. W., and Richter, W. (2001) *Micron 32*, 615−644.
29. Rinia, H. A., Kik, R. A., Demel, R. A., Snel, M. M. E., Killian, J. A., Van den Eerden, J. P. J. M., and De Kruijff, B. (2000) *Biochemistry 39*, 5852−5858.
30. Subczynski, W. K., Lewis, R. N. A. H., McElhaney, R. N., Hodges, R. S., Hyde, J. S., and Kusumi, A. (1998) *Biochemistry 37*, 3156−3164.
31. Zhang, Y.-P., Lewis, R. N. A. H., Henry, G. D., Sykes, B. D., Hodges, R. S., and McElhaney, R. N. (1995) *Biochemistry 34*, 2348−2361.
32. Harzer, U., and Bechinger, B. (2000) *Biochemistry 39*, 13106−13114.
33. Lewis, B. A., and Engelman, D. M. (1983) *J. Mol. Biol. 166*, 211−217.
34. Killian, J. A., and De Kruijff, B. (1985) *Biochemistry 24*, 7881−7890.
35. De Kruijff, B. (1987) *Nature 329*, 587−588.
36. Yau, W.-M., Wimley, W. C., Gawrisch, K., and White, S. H. (1998) *Biochemistry 37*, 14713−14718.
37. Persson, S., Killian, J. A., and Lindblom, G. (1998) *Biophys. J. 75*, 1365−1371.
38. McClellan, A. L. (1963) *Tables of Experimental Dipole Moments*, W. H. Freeman, San Francisco.
39. Demchenko, A. P. (1986) *Ultraviolet Spectroscopy of Proteins*, pp 5−26, Springer-Verlag, New York.
40. Mishra, V. K., Palgunachari, M. N., Segrest, J. P., and Anantharamaiah, G. M. (1994) *J. Biol. Chem. 269*, 7185−7191.
41. Mishra, V. K., and Palgunachari, M. N. (1996) *Biochemistry 35*, 11210−11220.
42. Strandberg, E., Morein, S., Rijkers, D. T. S., Liskamp, R. M. J., Van der Wel, P. C. A., and Killian, J. A. (2002) *Biochemistry 41*, 7190−7198.
43. Wimley, W. C., and White, S. H. (1996) *Nat. Struct. Biol. 3*, 842−848.

BI0257686